Buoy Analysis in a Point-Absorber Wave Energy Converter

Aldo Ruezga and José M. Cañedo C., *Member, IEEE*

***Abstract*—In this paper, a single-body point absorber system is analyzed to enhance its power absorption performance. The wave energy converter consists of a single floating body coupled to a direct-drive power takeoff system placed on the seabed. The geometry of a cylindrical buoy with large draft is modified, obtaining a particular geometry that is used to enhance the power absorption of the wave converter at a given site and at a finite depth. A numerical analysis tool (NEMOH) is used to obtain the buoy's frequency-dependent hydrostatic parameters; in addition, the buoy's dimensions are parameterized to tune the natural frequency of the oscillating system toward the frequency of dominant incident waves, thus enhancing wave power absorption for a specific wave frequency range. Furthermore, the damping influence of the power takeoff system on the performance of the wave energy converter is also considered.**

***Index Terms*—Point absorber, renewable energy, wave energy.**

I. Introduction

In recent years, ocean wave energy has become increasingly relevant to the global renewable energy outlook. Among the renewable energy sources, ocean waves have a higher power density than wind energy and they represent a great energy source with less intermittency [1].

To harness energy from ocean waves, several wave energy converters (WECs) have been developed by different institutions and companies [3]–[8], and the European Marine Energy Centre (EMEC), Stromness, U.K., has categorized these into eight WEC types. These devices utilize different kinds of power takeoff (PTO) systems to transform wave energy and are capable of harvesting wave energy from the shoreline and from deeper waters (offshore) [2], [3].

Due to their symmetry axes, point absorber and submerged pressure differential devices are the only WECs capable of extracting wave energy from all directions. Therefore, they need not be oriented toward incident waves. Furthermore, differential pressure devices perform better in the presence of large wave amplitudes and long wave periods, whereas point-absorber devices perform better in ocean waves with small amplitudes and short periods [12].

Manuscript received December 18, 2017; revised July 31, 2018 and November 30, 2018; accepted December 20, 2018. Date of publication January 31, 2019; date of current version April 14, 2020. This work was supported by Consejo Nacional de Ciencia y Tecnología (CONACYT), México. *(Corresponding author: Aldo Ruezga.)*

Associate Editor: M. A. Atmanand.

The authors are with the Centro de Investigación y de estudios Avanzados (CINVESTAV), Unidad Guadalajara, Zapopan 45019, México (e-mail: aruezga@gdl.cinvestav.mx; canedoj@gdl.cinvestav.mx).

Digital Object Identifier 10.1109/JOE.2018.2889529

Point absorbers are oscillating systems with axisymmetric bodies; they obtain energy from the vertical displacement of the water free surface. Physically, they are short in comparison to the incident wavelength (λ). These types of WECs are characterized by a narrow bandwidth [13], [15], [16], and their natural frequency does not usually coincide with the frequency of dominant ocean waves [3], [7], [16]. Therefore, to provide an optimum performance, the natural frequency of the oscillating system must be in tune with the incident wave frequency [3], [13], [15], [29]. Under resonance condition, the movement and absorbed power of the WEC device are maximized.

A variety of control techniques have been proposed to enhance performance in point absorber WEC devices. The control objective of these techniques is to maximize the power absorbed through an optimum phase condition, where buoy velocity should be in phase with the exciting force of the incident waves [3], [17]. A continuous phase control, known as reactive power control, requires that the power flow of the PTO system be reversed during some intervals of the WEC oscillating cycle [15], [16]; as a drawback, the PTO system must be able to supply energy to the oscillating system. As an alternative, suboptimal control methods are used to solve this inconvenience; these methods belong to discrete control techniques and do not need a reverse power flow in the PTO system. One of the most widely used is latching control, that works as follows: When the buoy velocity drops to zero, the buoy movement is held at its maximum excursion by a clamping mechanism or a hydraulic valve, and the buoy is released after a determined interval of time [15]–[19], such that its velocity is sufficiently in phase with the exciting force. However, latching control requires predicting incident waves.

If the WEC is properly sized, WEC performance is enhanced and the control requirements can be lowered. For this reason, several studies have focused on analyzing various sizes and shapes of floating bodies, with cylindrical, spherical, conical, and hemispherical forms being the most common.

For a single-body point absorber system, it was reported that a cylindrical buoy with a rectangular cross section provides a greater power absorption than other cross sections [20]. To maximize buoy displacement and power absorption at resonance with incident waves, Stelzer and Joshi [21] and Sjökvist *et al.* [22] analyzed a cylindrical buoy with various drafts and diameters, finding that as their size increases, their natural frequency is displaced toward lower frequencies; this is also described in [15]. Furthermore, the buoy's hydrostatic parameters increase as the water-plane area increases, whereas an increase in buoy

draft increases the added mass but decreases radiation damping. Conical and hemisphere bottom shapes were analyzed in [23] and [24], where main buoy diameter and buoy draft were evaluated at different values. Their results show that a conical bottom shape provides a better power absorption than a hemisphere shape. A similar analysis is made in [25]; their results show that a hydrodynamic buoy provides a lower added mass and radiation damping.

If the WEC structure so permits, mechanical elements can be added to adjust the natural frequency of the oscillating system. In [23] and [26], a supplementary mass is utilized to add inertia to the oscillating system, increasing absorption power. This component is placed on a moving mechanism that couples the buoy's movement to the PTO system, whereas in [27] and [28] an auxiliary mechanical system is utilized to provide an extra mechanical load, tuning the system's natural frequency. These point-absorber WEC systems are placed on a structure above the water surface, and the buoy is coupled to the PTO system by a rigid pillar. Depending on the mechanism added, cost and maintenance requirements could increase with this method.

In a two-body oscillating system, a floating body reacts to a submerged body used as a reference. Usually, the dynamics of both floating bodies are rigidly coupled by a hydraulic PTO system that converts the wave energy from the relative motion between both bodies [3], [9]–[11]. One drawback of hydraulic PTO systems is a delay in the time response; this is not present in direct-drive PTO systems. The two-body point absorber system analyzed in [32] consists of a conical buoy attached to a submerged water-mass vessel and a horizontal plate that provides a high inertia, which helps to reduce buoy size and tune the system's natural frequency, but reduces the exciting force. The buoy's heaving motion is damped by the hydraulic PTO system, which absorbs the wave energy. Blanco *et al.* [33] sized a two-body point absorber device that uses a direct-drive PTO system, obtaining large values for both body dimensions.

To enhance power absorption capabilities in a point absorber system, a single-body point-absorber WEC system was adapted to operate as a two-body oscillating system by Uppsala University, Uppsala, Sweden [29], [30]; this system is also analyzed in [31]. A neutrally buoyant spherical buoy is submerged between the primary floating body and the direct-drive PTO system placed on the seabed. The second body adds inertia to the oscillating system, shifting the natural frequency and increasing the capture width ratio (CWR) of the WEC system. Both bodies are placed at a determined distance to avoid hydrodynamic interference due to movement, requiring an increased water depth. Furthermore, if the point absorber system is properly tuned to incident waves, the required optimal PTO damping value can be lowered [29].

Adding inertia to the oscillatory system helps to adjust its natural frequency to dominant incident waves at the operation site. This can be done by adjusting buoy dimensions (draft and radius) to increase hydrostatic parameters; thus, a particular buoy shape is used to enhance system performance at a specific water depth, maximizing its power absorption.

Commonly, in a single-body point absorber system with a direct-drive PTO system placed at seabed, a large buoy is used to tune its natural frequency toward incident wave frequencies. A buoy with a large draft and volume provides a small amplitude of radiation damping with a narrow bandwidth. Therefore, it is decided to reduce the buoy volume to increase its frequency dependent hydrostatic parameters at a given water depth, improving the performance of the oscillating system.

A buoy of cylindrical shape with large draft is modified to reduce its volume, whereas the wetted surface is increased by changing some parts of its geometry, obtaining a single buoy with a shape similar to some two-buoy oscillating systems, where a secondary object helps to increase system inertia. The lower geometry is used to increase the added mass, as the radiation damping amplitude is maintained as high as possible.

It is widely known that water depth and wave resources available at the installation site influence the WEC design. This affects the buoy's hydrostatic parameters and WEC performance; therefore, a WEC device will not have the same performance when placed in a site with a different water depth and sea states. In most studies into WECs, sea states characterized by high-amplitude, long-period waves are usually used. In this paper, a single-body point-absorber system is designed to operate along Mexican coastlines in the Pacific Ocean, where the sea states are characterized by short-period waves and the wave energy resource is low in comparison to other places around the world.

II. Frequency Domain Model

Linear wave theory is used to model the WEC. This theory assumes that the free-surface displacement (η) is smaller than the wavelength (λ), and that the wavelength is greater than the buoy radius (r_b). In addition, the effects of small waves, such as diffraction, are neglected [14], simplifying system modeling and analysis.

A point absorber can be modeled as an equivalent mass-spring-damping system [36]; the device is restricted to moving one degree of freedom on the z-axis. The dynamic equation of the oscillating system is

$$m_b \ddot{z} = F_e + F_r + F_b + F_u \tag{1}$$

where m_b is the buoy mass, and the terms F_e, F_r, F_b, and F_u correspond to the excitation force, radiation force, buoyancy force, and an external force, respectively.

The excitation force is the force induced in the floating body by incident waves. Buoyancy force is affected by a buoyancy stiffness (S_b), composed of the buoy's water-plane area (A_{wp}), water density (ρ), gravity acceleration (g), and buoy displacement (z)

$$F_b = -\rho\, g\, A_{\mathrm{wp}} z = -S_b z. \tag{2}$$

External forces included in the term F_u are represented as a linear damping coefficient multiplied by the floating buoy velocity ($\dot{z}$)

$$F_u = -B_u \dot{z}. \tag{3}$$

The radiation force is defined by a radiation impedance that is composed of a radiation damping (B_3) and an added mass (m_3)

$$F_r = -\left[B_3(\omega) + i\omega\, m_3(\omega)\right] \dot{z}. \tag{4}$$

Radiation damping tends to zero as the frequency approaches infinity or zero, whereas the added mass is finite in both limits. These parameters are related to buoy motion in the water and do not depend on incident waves.

Replacing the force terms (2–4) in (1) and rearranging the equation gives the expression for the buoy's vertical movement

$$z = \frac{F_e}{-\omega^2 \left[m_b + m_3(\omega)\right] + i\omega \left[B_3(\omega) + B_u\right] + S_l}. \quad (5)$$

Stiffness S_l can include buoyancy stiffness (S_b) and moorage elements, and B_u is a damping due to an external system (e.g., a PTO system). Dividing (5) by the wave amplitude gives the response amplitude operator (RAO), which is a dimensionless transfer function that describes the vertical displacement of the device along the frequency range of incident waves. The displacement velocity is [36]

$$\dot{z} = u = \frac{F_e}{B_3(\omega) + B_u + i\left[\omega\, m_b + \omega\, m_3(\omega) - S_l/\omega\right]}. \quad (6)$$

Damping of the PTO system has an important effect on the device's response in resonance. The useful power (average power absorption) that an oscillating system can obtain from waves is expressed as [22], [36]

$$P_a = 0.5\omega^2 B_u |z|^2 = 0.5\, B_u |u|^2. \quad (7)$$

The absorbed power can be expressed in terms of radiation damping and excitation force [20]

$$P_a = \frac{|F_e|^2}{8B_3} - \left| u - \left(\frac{F_e}{2B_3}\right)\right|^2 \frac{B_3}{2}. \quad (8)$$

The power that the WEC device can absorb from waves can be described by the CWR, obtained by dividing the average absorbed power by the incident wave power multiplied by the buoy capture width

$$\mathrm{CWR} = P_a / Jd. \quad (9)$$

Where the incident wave power is defined by water depth (h), wave number (k), waveheight (H), and wave frequency (ω) [36]

$$J = \frac{\rho g^2 A^2 D(kh)}{4\omega} = \frac{\rho g^2 H^2}{16\omega}\left[1 + \frac{2kh}{\sinh(2kh)}\right]\tanh(kh). \quad (10)$$

Theoretically, the maximum absorbed power of an oscillating system is equal to $P_{\max} = J\lambda/2\pi$, and the maximum absorption width $(d_{\max})$ is defined as the ratio between $\mathrm{P}_{\max}$ and J [1], [36]

$$d_{\max} = \lambda/2\pi. \quad (11)$$

III. Analysis of the Buoy Geometry

The WEC's design has a profound influence on system performance, and the floating body dimensions (length and draft) and the water depth at the installation site affect its hydrostatic coefficients (added mass, radiation damping, and excitation force). Additionally, the WEC's design includes the influence of a PTO system, the restrictive elements, and the wave climate at a specific location to provide a good performance [2].

TABLE I
Wave Characteristics and Buoy Dimensions

Wave period T [s]	Wavelength λ [m]	Absorption width d [m]
4	24.9808	3.9758
5	39.0079	6.2083
6	55.8050	8.8816

To analyze the performance of the oscillating system, it is necessary to obtain the frequency-dependent hydrostatic parameters of the floating body. There are several specialized software programs for calculating hydrostatic coefficients of a particular geometric model; a comparison between WAMIT and NEMOH software is carried out in [37], showing a good agreement between them. Open source software NEMOH is used in this paper. This numerical tool uses the boundary element method (BEM) to compute the first-order wave loads on offshore structures (added mass, radiation damping, and wave forces) [38].

The WEC sizing process begins with the selection of wave parameters at a particular site. In this paper, the WEC device is placed at a water depth of 25 m, with a waveheight of 1 m (0.5 m wave amplitude) and wave periods ranging from 4 to 6 s. These wave parameters are associated with some sites along Mexican coasts in the Pacific Ocean [35].

It is known that dominant wave periods at the WEC operation site influence the buoy diameter selection; in a point absorber device, buoy diameter has an impact on power absorption—as buoy radius increases, power absorption rises [23]. Buoy radius is related to WEC absorption width and is calculated from (11) for each representative wave period (see Table I).

First, considering a typical cylindrical buoy and wave periods from 4 to 5 s, the buoy's diameter is selected as the average value of the absorption width related to both wave periods, resulting in a buoy diameter of 5 m. Analysis of the buoy's geometry is carried out for 40 angular frequencies in a range from 0.05 to 4 rad/s, and the draft length is evaluated in a range from 0.5 to 2 m. Hydrostatic parameters are shown in Fig. 1.

Draft has a crucial influence upon radiation damping; as the draft rises, the radiation damping amplitude decreases and tends to zero at lower frequencies, whereas the excitation force decreases its amplitude along the frequency band; this behavior is also shown in [23].

In a single-body point-absorber WEC, composed of a floating body directly coupled to a direct-drive PTO system placed on the seabed, wave movement is directly transferred to a linear electric generator suitable for use in point-absorber systems to avoid the use of gearboxes or similar elements that convert translational motion into rotary motion [34]. Generator dynamics are not taken into account, and their influence on the WEC systems is represented by a constant damping value.

A PTO damping value of 20 kN · s/m is used to determine WEC performance; this damping value is related to a 10-kW linear generator moving at 0.7 m/s [39]; additionally, a restoring coefficient (k_s) of 5 kN/m is used.

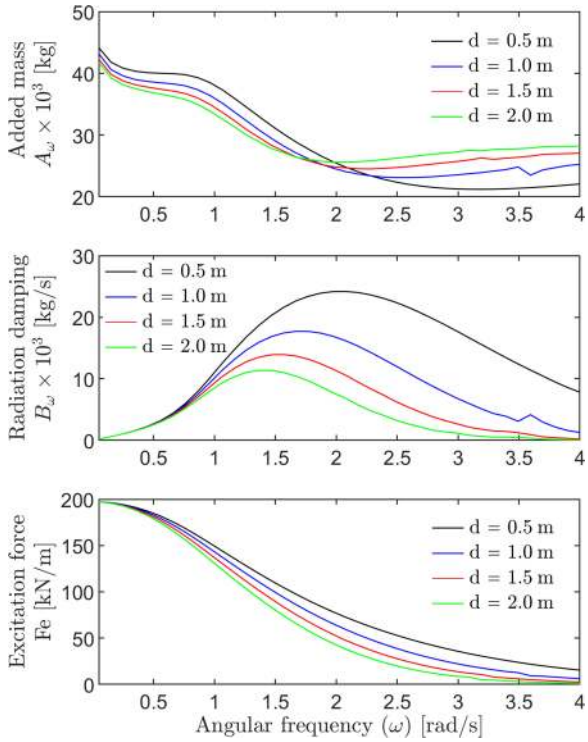

Fig. 1. Hydrostatic coefficients of a cylindrical buoy with different draft length. 2.5-m buoy radius, 25-m water depth.

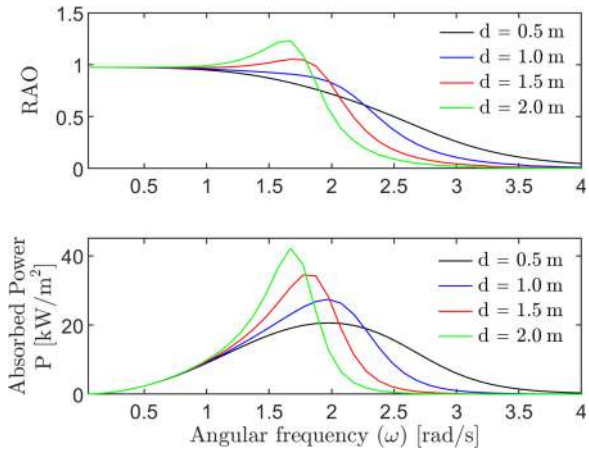

Fig. 2. RAO and absorbed power, 25-m water depth, 2.5-m cylindrical buoy radius.

The buoy's RAO and the absorbed power, obtained from (5) and (7), are shown in Fig. 2. A smaller draft provides a wider bandwidth, while a bigger draft reaches a higher absorbed power with a narrower frequency range. If the floating body provides a smaller radiation damping, the ability of the WEC device to radiate waves is decreased and the WEC's bandwidth is narrowed. The volume of the cylindrical buoy increases as it draft rises; therefore, buoy mass and system inertia also increase. In addition, the system's natural frequency is shifted toward smaller frequencies.

To enhance buoy performance in wave energy absorption, and based on two-body oscillating systems, in which a second object

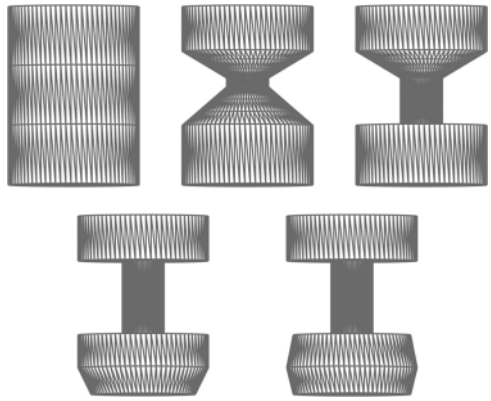

Fig. 3. Some changes made on the buoy sections.

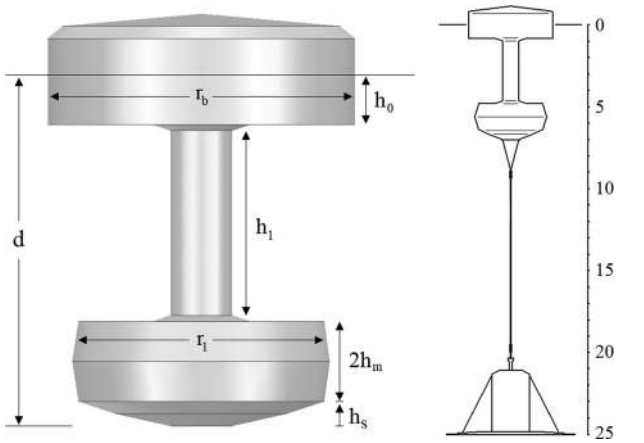

Fig. 4. (Left) Parameterized buoy geometry. (Right) Single-body point-absorber WEC system.

adds inertia to the oscillating system, a buoy with cylindrical shape is modified in this paper by changing some parts of its lower geometry.

To increase the added mass and maintain the radiation damping as high as possible, a cylindrical geometry is divided into three sections, as shown in Fig. 3. The top geometric section is maintained cylindrical, having a rectangular cross section near to the water-free surface and keeping a constant water-plane area, related to absorption width of the point-absorber WEC. However, several changes were made to the middle section, from reducing its radius to using conical shapes. The shape of the bottom was also modified, beveling its edges and changing its bottom from a flat to a semihemispherical shape. After analyzing the hydrostatic parameters of different geometrical combinations, the buoy geometry shown in Fig 4 provided a better improvement of the frequency dependent hydrostatic parameters.

Using a parameterizing process, buoy dimensions are evaluated using different values to tune the natural frequency of the oscillatory system to a frequency within the range of significant incident waves. The upper section is maintained as short as possible, but long enough to keep the buoy in contact with the water surface while moving under resonance conditions. The second section is composed of a tubular geometry that connects the top and bottom structures; the smallest possible radius is

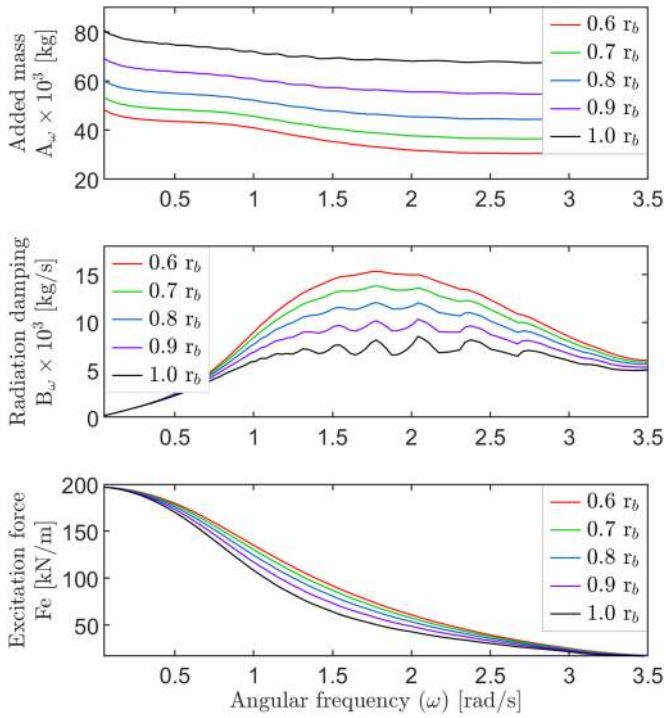

Fig. 5. Hydrostatic parameters for different radius values of the lower buoy geometry (r_1).

selected to reduce its influence on radiation damping while still providing sufficient structural support. The third section, with a semihemispherical bottom, helps to increase the added mass; but also has a significant influence on radiation damping. Therefore, its dimensions must be selected to maintain radiation damping as high as possible, as buoy performance is enhanced for the specified frequency range.

The diameter of the top section is maintained at 5 m. In the second section, length h_1 is evaluated in a range from 2 to 4 m, and its radius is evaluated in a range from 0.5 to 1 m; in the third section, height h_m is evaluated from 0.4 to 0.8 m and its radius r_1 is varied from 0.5 to 2 times the buoy radius (r_b). Hydrostatic coefficients are calculated in NEMOH software, buoy geometry is discretized into 4956 nodes and 1829 panels.

Analyzing the buoy parameters, it can be observed that if the radius of the third section is smaller than that of the top buoy section $(r_1 < r_b)$, then the hydrostatic coefficients maintain a certain balance; i.e., the added mass increases if $r_1 \geq r_b$, but radiation damping and excitation force decrease considerably. The best radius value for the bottom geometry (r_1) is determined to be in a range from 0.7 to 0.8 times the radius of the top geometry (r_b), Fig. 5.

The radius selected for the second buoy section is 0.5 m; a larger radius considerably affects the radiation damping amplitude and the range of frequencies at which it tends to zero. After sizing, the oscillating system is tuned to an undamped natural frequency of 1.48 rad/s approximately, corresponding to a wave period of 4.22 s.

The proposed modified buoy (MB) is compared to three cylindrical buoys with uniform cross sections (fixed radius) and draft lengths from 2 to 4 m, called C1, C2, and C3, respectively; these buoys are used as a reference and its parameters are shown in Table II. Fig. 6 shows a comparison between the frequency-dependent hydrostatic parameters. The MB provides a higher added mass; although this buoy has a larger draft in comparison with the 2-m draft cylindrical buoy C1, its radiation damping reaches a similar maximum amplitude and remains there for a wider frequency range.

TABLE II
BUOY PARAMETERS

Buoy	Radius r_b [m]	Draft d [m]	Volume V_b [m^3]	Mass M_b [kg]	Weight W_b [kN]
C1	2.5	2	39.2514	40232.6	394.6821
C2	2.5	3	58.8770	60349.0	592.0233
C3	2.5	4	78.5027	80465.3	789.3643
MB	2.5	7	42.5608	43624.8	427.9596

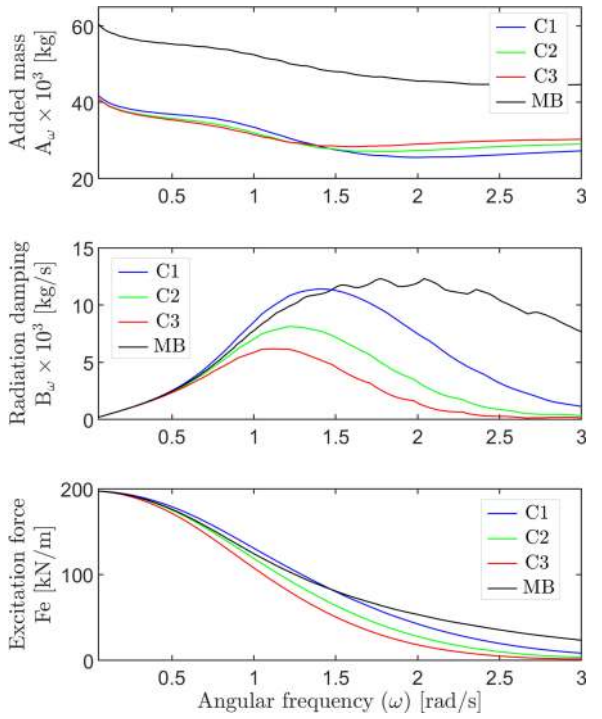

Fig. 6. Hydrodynamic coefficients; comparison between cylindrical buoys with different drafts and the MB.

A cylindrical three-meter draft buoy places the system's natural frequency in the incident-wave frequency range. Nevertheless, displacement and power absorption reach lower amplitudes at a narrower bandwidth than with the proposed buoy (see Fig. 7).

With the proposed geometry, buoy movement is approximately 1.84 times the wave amplitude at resonance frequency and reaches an absorbed power amplitude of approximately 70 kW/m^2; whereas buoy displacement is approximately 1.58 times the incident wave amplitude with the cylindrical buoy C2, with a maximum power of approximately 55 kW/m^2. In addition, the MB has a lower volume, mass, and weight.

A cylindrical 4-m draft buoy reaches a power magnitude of 65.4 kW/m^2 with a narrower bandwidth, and the system is tuned

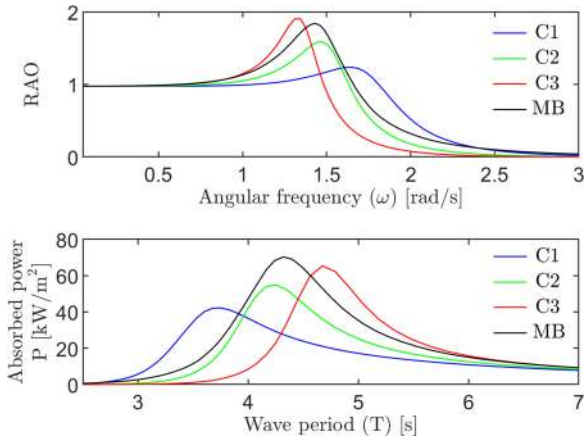

Fig. 7. RAO and absorbed power, PTO damp. 20 000 kg/s. Comparison between cylindrical buoys with different drafts and the MB.

TABLE III
BUOY DIMENSIONS AND CHARACTERISTICS

Buoy	r_b [m]	d [m]	h_m [m]	h_1 [m]	V [m^3]
MB_1	2.5	7.0	0.80	4	42.5608
MB_2	3.0	5.7	0.65	3	53.0414

BUOY PERFORMANCE

Buoy	ω_n [rad/s]	Absorbed power [kW/m^2]			RAO peak value
		T = 4s	T = 5s	T = $2\pi/\omega_n$	
MB_1	1.4880	47.33	35.37	70.32	1.838
MB_2	1.5006	55.03	32.10	71.56	1.832

B_u= 20 kN·s/m, k_s= 5 kN/m

to a lower frequency value; therefore, some required incident-wave frequencies are outside the bandwidth.

Additionally, the main buoy diameter (r_b) is increased from 5 to 6 m and the buoy geometry is parameterized again. As a result, buoy dimensions are reduced, decreasing buoy draft. Table III gives the dimensions of the buoy geometry after parameterization and buoy performance at three different wave periods.

In a direct-drive PTO system, PTO damping depends on the electric load fed by the electric system. This damping affects the WEC's ability to capture wave energy [39], [40]; therefore, if a control scheme is used in the PTO system, an adequate damping value could be useful for defining a reference signal to track and enhance WEC performance during operation. Furthermore, if a three-phase load connected at the generator terminals produces high currents in the armature winding, it develops high damping values, whereas a lower current produces low damping values [41]. PTO's damping influence on the system performance is analyzed using 19 damping values, ranging from 10 to 100 kN·s/m.

Considering the MB with diameters of 5 and 6 m, a maximum absorbed power is reached when the PTO system provides a damping value of 15 kN·s/m in buoy MB_1 and 20 kN·s/m in buoy MB_2; corresponding to peak power values of about 73.89

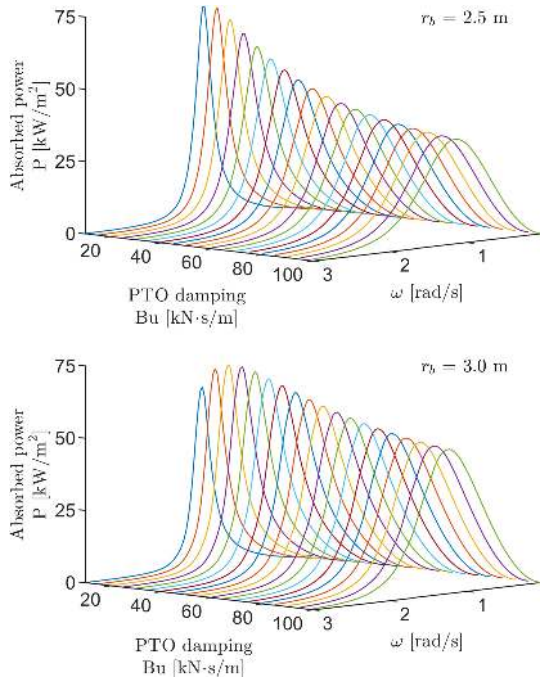

Fig. 8. Absorber power of the MB. (Above) 2.5-m radius, (below) 3-m radius.

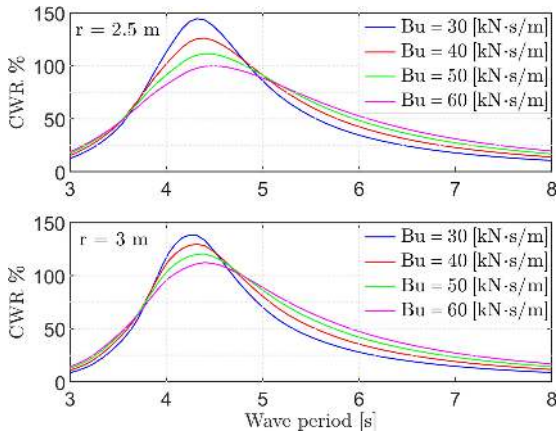

Fig. 9. CWR, incident wave amplitude of 0.5 m. (Above) Buoy radius 2.5 m, (below) Buoy radius 3.0 m.

and 71.56 kW/m^2, respectively. At these damping values, the WEC system has a narrower bandwidth (see Fig. 8). With larger damping values, the bandwidth is increased and the absorbed power amplitude is lowered.

Considering wave periods of 4 and 5 s, the absorbed power amplitudes are approximately 43.5 kW/m^2 at both wave periods when buoy MB_1 has an external damping value of 30 kN·s/m. In buoy MB_2, the external damping value required is 40 kN·s/m and the absorbed power is approximately 50 kW/m^2 at both points.

Buoy absorption efficiency is described by the CWR, which differs from converter device efficiency, obtained using (9), and the wave energy is calculated by expression (10), for a wave amplitude of 0.5 m. Fig. 9 shows the influence of PTO damping on the point absorber's CWR for both buoy diameters.

As PTO damping increases, the CWR decreases. For a PTO damping of 60 kN·s/m, buoy MB_1 has a CWR peak value of 100%, while the maximum value for buoy MB_2 is approximately 110%. If PTO damping is fixed at 40 kN·s/m, buoy MB_1 provides a CWR greater than or equal to 100% in a frequency range from 1.2885 to 1.5773 rad/s; the corresponding wave periods are 4.8764 and 3.9835 s. For buoy MB_2, the frequency range is from 1.3191 to 1.6002 rad/s and the wave periods are 4.7632 and 3.9265 s, respectively.

IV. Conclusion

A single-body point-absorber wave-energy converter is analyzed in frequency domain. For a finite water depth, a particular buoy geometry was dimensioned by analyzing its frequency-dependent hydrostatic parameters and the WEC performance in frequency domain, making it possible to define which buoy dimensions enhance hydrostatic parameters, thus improving WEC performance at finite water depths for a given sea state. Definition of the proposed buoy shape is based on two-body oscillating systems, and its dimensions were parameterized to tune the natural frequency of the oscillating system, improving its power absorption capability. In comparison with a large-draft cylindrical buoy with the same radius, the MB has a lower volume and mass. Moreover, it provides a higher added mass and radiation damping with a wider bandwidth.

Hydrostatic parameters are enhanced if the lower buoy radius (r_1) value is in a range from 0.7 to 0.8 times the buoy's main radius (r_b). Thus, added mass, radiation damping, and excitation force are maintained as high as possible for a large-draft buoy.

Furthermore, the damping influence of the PTO system on the WEC performance is analyzed using several damping values, although the dynamic of the PTO system is not considered. Damping analysis allows determining an adequate damping value that can be used as a reference signal in a control scheme to enhance power absorption.

A further analysis can be made to evaluate viscous losses to the oscillating system due to the drag force related to the buoy geometry used.

References

[1] J. Falnes, "A review of wave-energy extraction, Marine Structures, vol. 20, pp. 185–201, 2007, doi: doi.org/10.1016/j.marstruc.2007.09.001.

[2] J. Cruz, *Ocean Wave Energy: Current Status and Future Perspectives*. Berlin, Germany: Springer, 2007.

[3] A. F. de O. Falcão, Wave energy utilization: A review of the technologies, renewable and sustainable energy reviews, *Renewable Sustain. Energy*, vol. 14, pp. 899–918, 2010, doi: doi.org/10.1016/j.rser.2009.11.003.

[4] Ocean Energy Systems (OES), Ocean energy systems—Annual report, 2016. [Online]. Available: https://www.ocean-energy-systems.org/publications/annual-reports/document/oes-annual-report-2016/.

[5] M. Prado and H. Polinder, "Direct drive in wave energy conversion—AWS full scale prototype case study," in *Proc. IEEE Power Energy Soc. General Meeting*, Detroit, MI, USA, 2011, pp. 1–7, doi: 10.1109/PES.2011.6039720.

[6] A. Weinstein, G. Fredrikson, M. J. Parks, and K. Nielsen, "AquaBuOY—the offshore wave energy converter numerical modeling and optimization," in *Proc. Oceans '04 MTS/IEEE Techno-Ocean '04*, Kobe, Japan, 2004, vol. 4, pp. 1854–1859, doi: 10.1109/OCEANS.2004.1406425.

[7] J. P. Kofoed, P. Frigaard, E. Friis-Madsen, and H. C. Sørensen, "Prototype testing of the wave energy converter wave dragon," *Renewable Energy*, vol. 31, pp. 181–189, 2006, doi: doi.org/10.1016/j.renene.2005.09.005.

[8] R. Henderson, "Design, simulation, and testing of a novel hydraulic power take-off system for the Pelamis wave energy converter," *Renewable Energy*, vol. 31, pp. 271–283, 2006, doi: doi.org/10.1016/j.renene.2005.08.021.

[9] C. D. Engin and A. Yesildirek, "Designing and modeling of a point absorber wave energy converter with hydraulic power take-off unit," in *Proc. 4th Int. Conf. Elect. Power Energy Convers. Syst.*, 2015, pp. 1–6, doi: 10.1109/EPECS.2015.7368507.

[10] Ocean Power Technologies, Pennington, NJ, USA, 2018, [Online]. Available: https://www.oceanpowertechnologies.com/powerbuoy, Accessed: Nov. 2018.

[11] J. Weber, F. Mouwen, A. Parish, and D. Robertson, "Wavebob–research & development network and tools in the context of systems engineering," in *Proc. 8th Eur. Wave Tidal Energy Conf.*, Uppsala, Sweden, 2009.

[12] J. Faiz and M. Ebrahimi-Salari, "Comparison of the performance of two direct wave energy conversion systems: Archimedes wave swing and power buoy," *J. Mar. Sci. Appl.*, vol. 10, pp. 419–428, 2011, doi: 10.1007/s11804-011-1087-9.

[13] M. E. McCormick, "Ocean wave energy concepts," in *Proc. OCEANS '79*, 1979, pp. 553–558, doi: doi.org/10.1109/OCEANS.1979.1151266.

[14] M. McCormick, *Ocean Engineering Mechanics With Applications*. Cambridge, U.K.: Cambridge Univ. Press, 2009.

[15] J. Falnes and J. Hals, Heaving buoys, point absorbers and arrays, philosophical transactions of the royal society A: Mathematical, physical and engineering sciences, vol. 370, pp. 246–277, 2011, doi: doi.org/10.1098/rsta.2011.0249.

[16] J. Falnes, Optimum control of oscillation of wave-energy converters, in Annex Report B1: Device fundamentals/hydrodynamics of the wave energy converters: Generic technical evaluation study, Commission of the European Communities, Brussels, Belgium, 1993.

[17] J. Falnes, "Principles for capture of energy from ocean waves, phase control and optimum oscillation," *Norwegian J. Elektro*, vol. 111, no. 1, pp. 102–106, 1998.

[18] M. Greenhow and S. P. White, "Optimal heave motion of some axisymmetric wave energy devices in sinusoidal waves," *Appl. Ocean Res.*, vol. 19, pp. 141–159, 1997, doi: doi.org/10.1016/S0141-1187(97)00020-5.

[19] B. Teillant, J. C. Gilloteaux, and J. V. Ringwood, "Optimal damping profile for a heaving buoy wave energy converter," in *Proc. 8th IFAC Conf. Control Appl. Mar. Syst.*, 2010, vol. 43, pp. 360–365, doi: doi.org/10.3182/20100915-3-DE-3008.00067.

[20] T. Usha, "Power absorption by thin wave devices," *Appl. Math. Model.*, vol. 14, pp. 327–333, 1990, doi: doi.org/10.1016/0307-904X(90)90085-J.

[21] M. A. Stelzer and R. P. Joshi, "Evaluation of wave energy generation from buoy heave response based on linear generator concepts," *J. Renewable Sustain. Energy*, vol. 4, 2012, Art. no. 063137, doi: doi.org/10.1063/1.4771693.

[22] L. Sjökvist, R. Krishna, M. Rahm, V. Castellucci, A. Hagnestål, and M. Leijon,"On the optimization of point absorber buoys," *J. Mar. Sci. Eng.*, vol. 2, pp. 477–492, 2014, doi: doi.org/10.3390/jmse2020477.

[23] G. De Backer, Hydrodynamic design optimization of wave energy converters consisting of heaving point absorbers, Ph.D. dissertation, Dept. Civil Eng., Ghent Univ., Gent, Belgium, 2009.

[24] J. Pastor and Y. Liu, "Frequency and time domain modeling and power output for a heaving point absorber wave energy converter," *Int. J. Energy Environ. Eng.*, vol. 5, p. 101, 2014, doi: doi.org/10.1007/s40095-014-0101-9.

[25] S. Jin and R. Patton, "Geometry influence on hydrodynamic response of a heaving point absorber wave energy converter," in *Proc. 12th Eur. Wave Tidal Energy Conf.*, 2017. [Online]. Available: https://www.researchgate.net/publication/319464943_Geometry_Influence_on_Hydrodynamic_Response_of_a_Heaving_Point_Absorber_Wave_Energy_Converter

[26] M. Vantorre, R. Banasiak, and R. Verhoeven, "Modelling of hydraulic performance and wave energy extraction by a point absorber in heave," *Appl. Ocean Res.*, vol. 26, pp. 61–72, 2004, doi: doi.org/10.1016/j.apor.2004.08.002.

[27] A. Josefsson, A. Berghuvud, K. Ahlin, and G. Broman, "Performance of a wave energy converter with mechanical energy smoothing," in *Proc. Eur. Wave Tidal Energy Conf.*, 2011. [Online]. Available: http://www.diva-portal.org/smash/record.jsf?pid=diva2%3A834914&dswid=-4592

[28] A. H. Sakr, Y. H. Anis, and S. M. Metwalli, "System frequency tuning for heaving buoy wave energy converters," in *Proc. IEEE Int. Conf. Adv. Intell. Mechatronics*, 2015, pp. 1367–1372, doi: doi.org/10.1109/AIM.2015.7222729.

[29] J. Engström, M. Eriksson, J. Isberg, and M. Leijon, "Wave energy converter with enhanced amplitude response at frequencies coinciding with Swedish west coast sea states by use of a supplementary submerged body," *J. Appl. Phys.*, vol. 106, 2009, Art. no. 064512, doi: doi.org/10.1063/1.3233656.
[30] J. Engström, V. Kurupath, J. Isberg, and M. Leijon, "A resonant two body system for a point absorbing wave energy converter with direct-driven linear generator," *J. Appl. Phys.*, vol. 110, 2011, Art. no. 124904, doi: doi.org/10.1063/1.3664855.
[31] S. Bozzi, A. M. Miguel, A. Antonini, G. Passoni, and R. Archetti, "Modeling of a point absorber for energy conversion in Italian Seas," *Energies*, vol. 6, pp. 3033–3051, 2013, doi: doi.org/10.3390/en6063033.
[32] V. Ferdinande and M. Vantorre, "The concept of a bipartite point absorber," in *Hydrodynamics of Ocean Wave-Energy Utilization. International Union of Theoretical and Applied Mechanics*, D. V. Evans and A. F. O. de Falcão, Eds. Berlin, Germany: Springer, 1986, pp. 217–226, doi: doi.org/10.1007/978-3-642-82666-5_18.
[33] M. Blanco, M. Lafoz, and G. Navarro, "Wave energy converter dimensioning constrained by location, power take-off and control strategy," in *Proc. IEEE Int. Symp. Ind. Electron.*, 2012, pp. 1462–1467, doi: doi.org/10.1109/ISIE.2012.6237307.
[34] J. Brooke, *Wave Energy Conversion*. New York, NY, USA: Elsevier, 2003.
[35] A. I. Pérez Peña, Estimación del clima marítimo y la energía del oleaje disponible en las costas mexicanas, M.S. thesis, Facultad de Ingeniería Civil, Universidad Nacional Autónoma de México, Mexico City, Mexico, 2012.
[36] J. Falnes, *Ocean Waves and Oscillating Systems: Linear Interactions Including Wave-Energy Extraction*. New York, NY, USA: Cambridge Univ. Press, 2002.
[37] A. Roessling and J. Ringwood, *Finite Order Approximations to Radiation Forces for Wave Energy Applications, Renewable Energies Offshore*. Boca Raton, FL, USA: CRC Press, 2015, pp. 359–366.
[38] A. Babarit and G. Delhommeau, "Theoretical and numerical aspects of the open source BEM solver NEMOH," in *Proc. 11th Eur. Wave Tidal Energy Conf.*, 2015. [Online]. Available: https://hal.archives-ouvertes.fr/hal-01198800
[39] M. Eriksson, J. Isberg, and M. Leijon, "Hydrodynamic modelling of a direct-drive wave energy converter," *Int. J. Eng. Sci.*, vol. 43, pp. 1377–1387, 2005, doi: doi.org/10.1016/j.ijengsci.2005.05.014.
[40] R. Waters *et al.*, "Ocean wave energy absorption in response to wave period and amplitude – offshore experiments on a wave energy converter," *IET Renewable Power Gener.*, vol. 5, pp. 465–469, 2011, doi: doi.org/10.1049/iet-rpg.2010.0124.
[41] M. Eriksson, R. Waters, O. Svensson, J. Isberg, and M. Leijon, "Wave power absorption: Experiments in open sea and simulation," *J. Appl. Phys.*, vol. 102, 2007, Art. no. 084910, doi: doi.org/10.1063/1.2801002.

Aldo Ruezga was born in Guadalajara, Jalisco, Mexico, in 1986. He received the B.Sc. degree in mechanical and electrical engineering from the University of Guadalajara, Guadalajara, Mexico, in 2010 and the M.Sc. degree in electrical engineering from the Centro de Investigación y de Estudios Avanzados (CINVESTAV), Guadalajara, Mexico, in 2015, where he is currently working toward the Ph.D. degree.

His main interests are related to renewable energies.

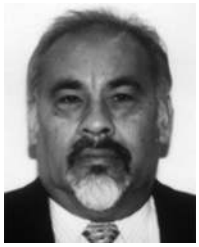

José M. Cañedo C. (M'96) was born in Mazatlán, Sinaloa, Mexico, in 1950. He received the B.Sc. degree in electrical engineering from the University of Guadalajara, Guadalajara, Mexico, in 1971, the M.Sc. degree in electrical engineering from the National Polytechnic Institute, Mexico City, Mexico, in 1980, and the Ph.D. degree in electrical engineering from the Moscow Power Institute, Moscow, Russia, in 1985.

From 1988 to 1994, he was a Researcher with CFE México, Mexico. From 1994 to 1997, he was with the University of Guadalajara, Guadalajara, Mexico, and since 1997, he has been a Professor for graduate programs in electrical engineering with CINVESTAV, Guadalajara, Mexico. His research interests include nonlinear robust control of power systems, electric machines, and renewable energies.